



Cite this: *RSC Adv.*, 2023, **13**, 34097

Received 29th September 2023  
 Accepted 13th November 2023

DOI: 10.1039/d3ra06647a  
[rsc.li/rsc-advances](http://rsc.li/rsc-advances)

## Introduction

Protein structure is very sensitive to their microenvironments.<sup>1</sup> Structural alteration of proteins is often observed due to several factors (modulators) like pH,<sup>2</sup> temperature,<sup>2</sup> salt concentration,<sup>3</sup> and different types of small molecules.<sup>4,5</sup> This change in the presence of physical and chemical modulators is significant because it may change the function of the proteins.<sup>6,7</sup> The study of the modulators' interactions with proteins has drawn attention from the scientific community.<sup>8,9</sup>

Human insulin is a protein hormone in the blood that regulates blood sugar levels.<sup>10,11</sup> Depending upon the exposure and availability of it in the body, several medical conditions like hypertension,<sup>12</sup> coronary heart disease,<sup>13</sup> stroke,<sup>14</sup> cancer,<sup>15</sup> and type II diabetes<sup>16</sup> are widespread nowadays. The small monomeric insulin contains fifty-one amino acids and is divided into two  $\alpha$ -helical structures, joined together by three disulfide bonds (intra-chain and inter-chain).<sup>17</sup> This small monomeric form of insulin is highly unstable.<sup>18,19</sup> Again, insulin is one of the serum proteins that commonly interact with the polar poly-hydroxyl group containing molecules like glucose. However, in the serum, many hydrophobic molecules can affect the structure and function of the insulin. Thus, the structure of insulin may change in the presence of diverse molecules in the blood and these

compound can initiate insulin-related diseases. Therefore, an investigation of the effect of molecules with hydroxyl groups and hydrophobic groups on the insulin's structure is highly essential.

Protein-small molecule interaction studies are used to investigate the structural effect on proteins in the presence of different microenvironments.<sup>20,21</sup> The tuning of the microenvironment is possible through the proper choice of small molecules.<sup>22,23</sup> Hydrophilic to hydrophobic molecules can be synthesized from simple organic reactions. The reaction of an aldehyde with primary amine is one of the simple organic reactions used to join two fragments through imine bond formation.<sup>24</sup> The products of the reaction are known as Schiff's base.<sup>24</sup> With the proper choice of the substituent attached to the amine and aldehyde part, the hydrophilicity and hydrophobicity of the molecule can be tunable. For this reason, Schiff's base is used in very diverse fields of science like coordination chemistry,<sup>25,26</sup> hydrogels,<sup>27,28</sup> sensing,<sup>29</sup> analytical chemistry, electronics, optics<sup>25</sup> etc.

In this study, we have synthesized one hydrophobic Schiff's base (*E*)-2-((*tert*-butylimino) methyl)-6-methoxyphenol and one hydrophilic Schiff's base (*E*)-2-((2-hydroxy-3-methoxybenzylidene) amino)-2-(hydroxymethyl)propane-1,3-diol. The interactions of these two molecules with insulin have been investigated here. Therefore, it will provide a scope to monitor the structure of insulin in two opposite microenvironments.

## Results and discussion

### Synthesis of Schiff's base and choice of compounds

Insulin binds with glucose, which is a polar poly-hydroxy compound. For this reason, a poly-hydroxy compound is

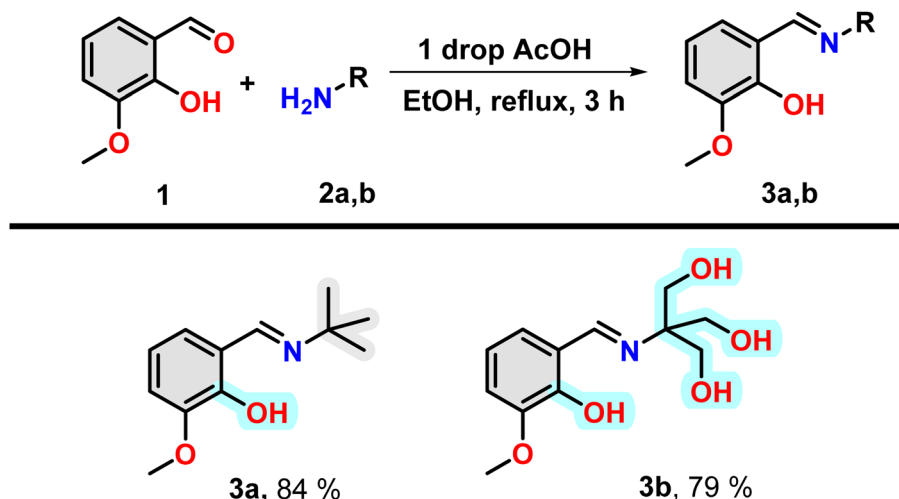
<sup>a</sup>Department of Chemistry, Jadavpur University, Kolkata-700032, India. E-mail: [juumesh.halder@gmail.com](mailto:juumesh.halder@gmail.com)

<sup>b</sup>Department of Chemistry, Lady Brabourne College, Kolkata-700017, India

<sup>c</sup>Department of Chemistry, College of Science, King Saud University, Riyadh 11451, Saudi Arabia

† Electronic supplementary information (ESI) available. See DOI: <https://doi.org/10.1039/d3ra06647a>





Scheme 1 Synthesis of Schiff base compounds **3a** and **3b**.

required to be designed in our study as one of the compounds. To understand the effect of binding a hydrophobic molecule to insulin, a similar molecule without the hydroxyl group has been designed. It is found that electron-rich aromatic molecules have unique protein binding ability. For this reason, the attachment of said poly-hydroxyl group containing and hydrophobic moiety with an aromatic moiety having a hydroxyl group separately will be one of the choices for the fulfilment of the target of investigation. For the easy joining of these two moieties, Schiff bases formation reaction is a convenient choice. Thus, two amine compounds 2-amino-2-(hydroxymethyl)propane-1,3-diol and 2-methylpropan-2-amine were selected for a poly-hydroxyl and hydrophobic moiety, respectively. Now, one electron-rich aldehyde is required for Schiff base formation. In this case, *ortho*-vanillin is the best because it contains one *ortho*-hydroxy and *meta*-methoxy group along with aldehyde at the benzene ring.

Under refluxing conditions in dry ethanol, the reaction between *ortho*-vanillin (**1**) and aliphatic amine (**2**) yielded corresponding Schiff bases. With the addition of one drop of glacial acetic acid, this reaction proceeded for three hours. When *tert*-butyl amine (**2a**) and 2-amino-2-(hydroxymethyl)propane-1,3-diol (**2b**) were employed in the reaction, high-yield production of compound **3a** and **3b** was achieved respectively (Scheme 1). The compounds were characterized through the use of <sup>1</sup>H NMR.

It is to be noted that the compound **3a** have one hydrogen bond forming group, *i.e.* hydroxyl group and have hydrophobic *t*-Bu group and an aromatic ring (grey highlighted). Therefore, the molecule is hydrophobic in nature. However, in the case of **3b**, the presence of three OH group in the nitrogen containing part instead of *t*-Bu group, make this region hydrophilic (cyan highlighted). Therefore, compound **3a** and **3b** will offer purely hydrophobic and largely hydrophilic environment in the vicinity of insulin.

#### Spectroscopic study of the Schiff base compounds

**UV-vis spectroscopy study.** The small molecule under investigation (**3a** and **3b**) show response in the UV-vis

spectroscopy and give peaks at 402, 285, and 232 nm for compound **3a** and 412, 292 and 237 nm for **3b** (Fig. S1†). To check the stability of the compounds in this solvent system, the compounds (**3a** and **3b**) were separately mixed into the solvent system, and UV-vis spectra were recorded with time. The results indicate that the compounds are stable in these conditions, as slight changes were observed during 3.5 h (Fig. S2†).

**Fluorescence study.** The investigating compounds also have fluorescence properties. Both compounds **3a** and **3b** produce three hump emission spectra with peaks at 322, 333, and 347 nm on excitation at 276 nm (Fig. S3†). The hydrophobic nature of **3a** can influence its aggregation-caused quenching (ACQ) or aggregation-induced emission (AIE) in water. To check this effect, we set an experiment where the compound was gradually added to the experimental conditions without insulin. The results show that the **3a** has ACQ (Fig. S4A and B†) at high concentration. However, at lower concentrations of the **3a** (insulin-compound interaction was observed in this concentration range), any type of self-aggregation of the compound is absent, which is evident from the linear relation between concentration and fluorescence intensity. This linear behavior breaks after 25  $\mu$ M and follows a polynomial curve, which indicates their self-aggregation in the experimental solvent system.

The **3b** is a hydrophilic molecule, and it shows self-aggregation in the experimental conditions at high concentrations. In this case, the compound shows aggregation-induced emission as the fluorescence intensity increases slowly with **3b** concentration (Fig. S4C and D†). However, at low concentrations (2–25  $\mu$ M), there is also a linear relation between concentration and **3b** fluorescence intensity. Therefore, at lower concentrations of both compounds, the self-aggregation of them cannot proceed rapidly.

#### Study of interactions of the Schiff bases with human insulin

**UV-vis spectroscopy study.** The ultraviolet-visible spectroscopic can be employed to understand the environment of the chromophore of the protein or small molecules during their



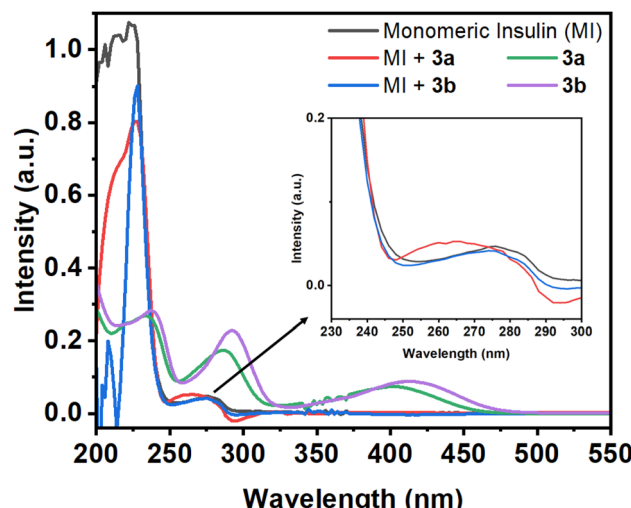


Fig. 1 Absorption spectra of monomeric insulin (10  $\mu$ M in pH 2.0) in the absence and presence of Schiff base compounds **3a** and **3b**. Absorption spectra of **3a** and **3b** (50  $\mu$ M in pH 2.0).

interaction. In this work, we have chosen the insulin as a model protein where *p*-hydroxyphenyl group in the Tyr residue acts as a chromophore. Monomeric insulin contains four Tyr residues and shows a peak at  $\lambda_{\text{max}} = 276$  nm (Fig. 1).

If the environment of the Tyr residues of protein changes during the interactions with small molecules, then the nature of this peak may changes. In the presence of the compound **3a**, the 276 nm peak of the protein show a blue shift of 11 nm with the enhancement of the intensity. However, in the case of compound **3b**, the protein peak shows slight blue shift of 2 nm. Although, the compounds have peak at 286 and 289 nm for **3a** and **3b**, respectively, but the protein peak (276 nm) shows blue shift upon addition of compounds. From this initial study, it may be assumed that the compounds can have capability to interact with the protein.

#### Intrinsic fluorescence study of insulin in presence of Schiff base compounds

The Tyr residues of the monomeric insulin also show an emission response and give an emission peak at 304 nm on excitation at

Table 1 The Stern–Volmer ( $K_{\text{sv}}$ ) and binding ( $K_b$ ) constant of **3a** and **3b** at different temperature

Compound	$K_{\text{sv}}, 10^4 (\text{M}^{-1})$			$K_b, 10^4 (\text{M}^{-1})$		
	283 K	293 K	303 K	283 K	293 K	303 K
<b>3a</b>	4.99	3.94	3.65	2.83	2.18	1.65
<b>3b</b>	6.64	7.47	8.64	16.08	17.09	18.57

276 nm. Upon addition to the **3a** in the monomeric insulin solution (25  $\mu$ M) at 283 K, the peak intensity of insulin (304 nm) decreases rapidly with a 7 nm red shift (Panel A, Fig. 2). The appearance of the peak at 312 nm with the addition of the compound is the characteristic of the compound **3a**. In the case of compound **3b**, a similar type of observation was found at the same temperature (Panel B, Fig. 2). The intensity of the said protein peak was decreased with the gradual addition of the compound.

Stern–Volmer equation can be used to determine the affinity of compounds to bind to proteins.

$$I^0/I = 1 + K_{\text{sv}}[C] \quad (1)$$

Here, initial protein fluorescence intensity ( $I^0$ ) and intensity ( $I$ ) after the addition of compounds **3a** and **3b**. This quenching constant ( $K_{\text{sv}}$ ) is a measurement of the strength of the interaction between the compound and the protein. The slope of the plot of  $I^0/I$  vs.  $C$  is related to the quenching constant and can be used to calculate the quenching constant. In order to analyze fluorescence quenching, the Stern–Volmer eqn (1) was used, and Table 1 provides the quenching constants for different temperatures (Fig. 3). As can be seen in Table 1, the results indicate that the  $K_{\text{sv}}$  for **3a** is inversely proportional to the temperature, while for **3b**, it has been found to have a direct correlation with the temperature. Consequently, it implies that these compounds bind to proteins in different ways depending on the binding mechanism that they use.

#### Binding parameters

By evaluating the binding constant ( $K$ ) and the change in free energy ( $\Delta G$ ) of the synthesized compounds–insulin interaction,

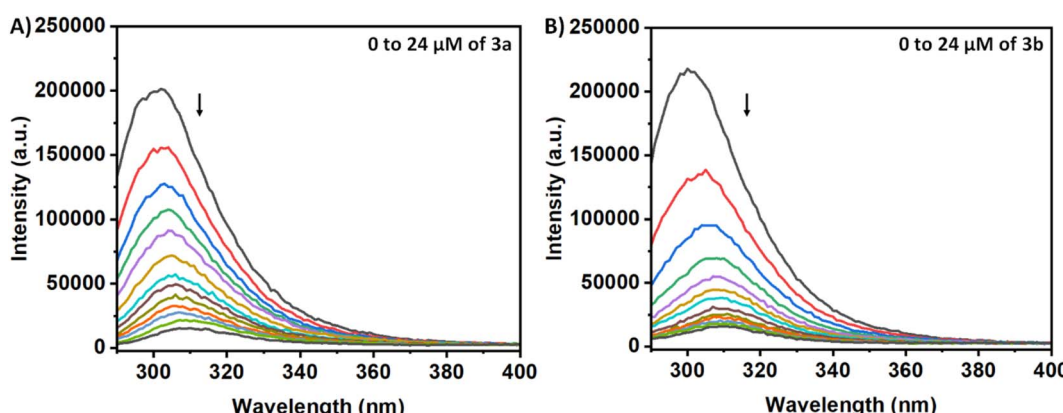


Fig. 2 Fluorescence spectral change of insulin on gradual addition of (A) **3a** and (B) **3b**.



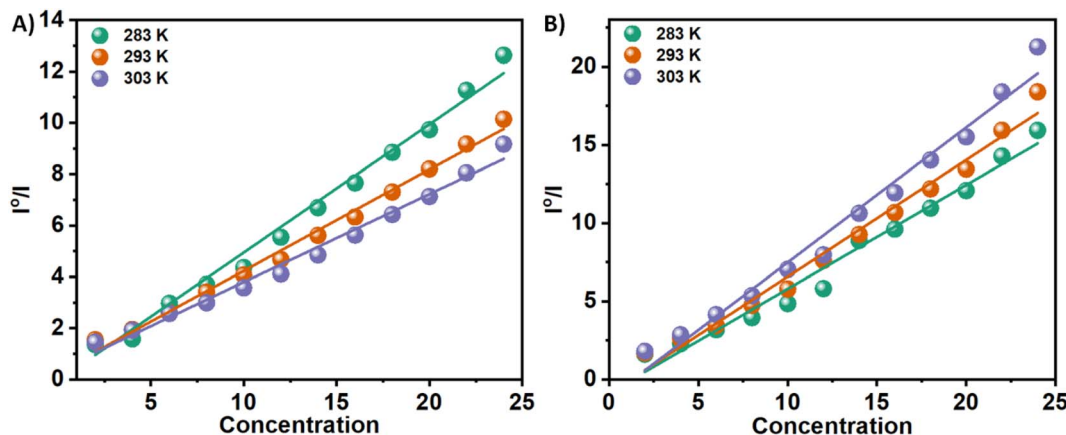


Fig. 3 Stern–Volmer plots for the quenching of Tyr-fluorescence of insulin at 283, 293, and 303 K in the presence of two Schiff base **3a** (Panel A) and **3b** (Panel B) in solution.

we can quantify the interaction between small molecules (**3a** and **3b**) and protein. A fundamental aspect of the efficacy of small molecules lies in their ability to bind to the target protein, as well as their subsequent effect on its stability. This significantly affects binding efficacy. In order to determine the quantitative assessment of  $K$  and  $\Delta G$ , the following equation is used to analyze the fluorescence quenching data. When a pair of complimentary species bind independently to equal sites in a macromolecule, this equation describes the equilibrium between the free and bound species.

$$\ln((I^0 - I)/I) = \ln K_b + n \ln[C] \quad (2)$$

$n$  is the number of binding sites, and  $K_b$  is the binding constant. There have been extensive studies in the literature utilizing the above eqn (2) to elucidate binding parameters from fluorescence quenching data as a method for predicting binding parameters. Table 1 summarizes the results of this study, conducted at various temperatures. Fig. 4 shows representative plots of  $\ln((I^0 - I)/I)$  versus  $\ln[C]$ , which is a measure of how protein–compound interactions were affected by

temperature. The results also indicate that the binding of **3a** is weaker than that of **3b**. Therefore, insulin has more preference to bind with the polar molecules in contrast with the hydrophobic molecules. The binding of the **3a** to the insulin decreases with increasing temperature. However, reverse phenomenon was found in the case of **3b**.

#### Binding forces and thermodynamic parameters

In a broader sense, the interactions between small molecules and biomolecules can be summed up as having many different types of forces. A variety of forces interact within an interacting site, including electrostatic forces, hydrogen bonds, van der Waals interactions, and hydrophobic and steric contacts. Traditionally, to account for the principal forces of binding between small molecules and proteins, the signs and magnitudes of thermodynamic parameters have been invoked. By taking into account the assumption that there is no significant change in the enthalpy change ( $H$ ) over a particular temperature range, the enthalpy change ( $H$ ) and the entropy change ( $S$ ) can both be calculated from the following van't Hoff equation:

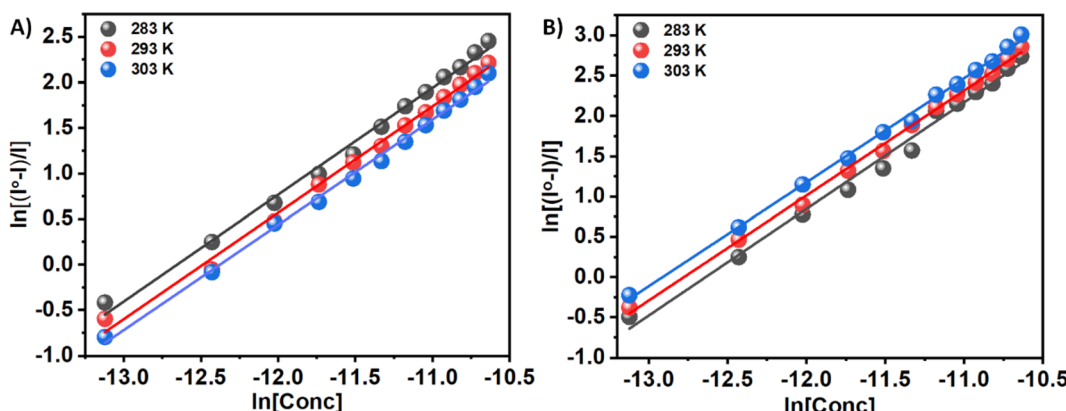


Fig. 4  $\ln((I^0 - I)/I)$  versus  $\ln[C]$  plots for the quenching of Tyr-fluorescence of insulin at 283, 293, and 303 K in the presence of two Schiff base **3a** (Panel A) and **3b** (Panel B) in solution.



**Table 2** Thermodynamic parameters involved in the insulin–3a/3b interactions

Compounds	Temperature (K)	$\Delta G^\circ$ kJ mol <sup>-1</sup>	$\Delta H^\circ$ kJ mol <sup>-1</sup>	$\Delta S^\circ$ kJ mol <sup>-1</sup>
3a	283	−5.41		
	293	−5.98	+10.72	+0.057
	303	−6.55		
3b	283	−12.16		
	293	−11.33	−35.65	−0.083
	303	−10.50		

$$\ln K = \Delta H/RT + \Delta S/R \quad (3)$$

In this case,  $R$  represents the universal gas constant and  $T$  represents the Kelvin temperature. The free energy change ( $\Delta G$ ) resulting from the process in this case is then estimated by using the relationship given below:

$$\Delta G = \Delta H - T\Delta S \quad (4)$$

There are several thermodynamic parameters that can be calculated and listed in Table 2, and a representation of the van't Hoff plot ( $\ln K$  vs.  $1/T$ ) can be found in Fig. 5.

Several kinds of interaction occur during protein–small molecule interaction. There is a link between these interactions and the thermodynamic parameters previously documented by Ross and Subramanian. These parameters have provided insights into the mechanisms by which each interaction occurs. According to the thermodynamic data, the following can be summarized as the model of interaction on the basis of the data related to the interaction:

- (i)  $\Delta H > 0$ ,  $\Delta S > 0$  correspond to hydrophobic forces.
- (ii)  $\Delta H < 0$ ,  $\Delta S < 0$  correspond to hydrogen bond formation and van der Waals interaction.
- (iii)  $\Delta H < 0$ ,  $\Delta S > 0$  correspond to electrostatic/ionic interactions.

It has been demonstrated that the enthalpically unfavorable and entropically favorable thermodynamic parameters for the interaction between 3a and insulin are presented in Table 2, with a negative Gibbs free energy change, suggesting that the interaction may occur spontaneously. However, with a negative Gibbs free energy change, the 3b–insulin interaction is enthalpically favorable and entropically unfavorable. It should be noted that the positive enthalpy and entropy change demonstrate that the interaction process between 3a and insulin is dominated by hydrophobic forces. Again, 3b and insulin interact through hydrogen bond formation and van der Waals interaction, as demonstrated by the negative enthalpy and entropy changes.

### Monitoring the hydrophobicity changes in the microenvironment of insulin: ANS assay

8-Anilinonaphthalene-1-sulfonic acid is a fluorescent probes having higher fluorescence intensity when binds at the hydrophobic pocket of the protein surface (also for insulin)<sup>30–33</sup> with

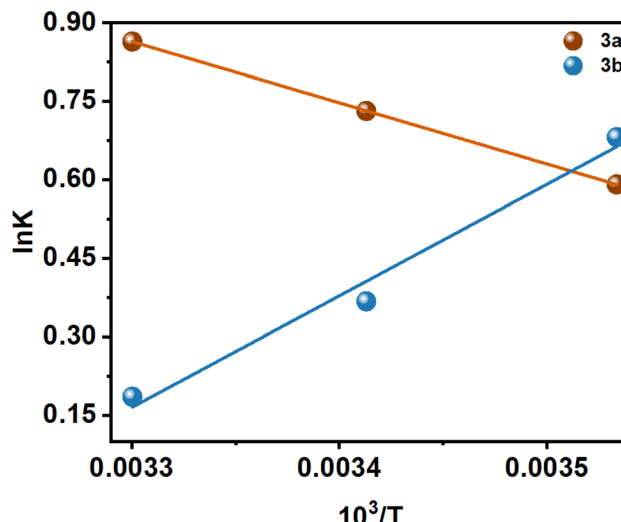


Fig. 5  $\ln K$  vs.  $1/T$  plot at 283, 293, and 303 K of two Schiff base 3a and 3b.

respect to its unbound state. Therefore, if one compounds able to displace ANS from the binding site of the protein, then the intensity of the ANS bound insulin will decrease. The results will indicate the said compound can bind at the hydrophobic site of the protein surface. In the case of the compound 3a, the intensity of the ANS–insulin system decrease with the gradual addition of it (Panel A, Fig. 6). However, for 3b, the decrease of fluorescence intensity is low with addition of the compound (Panel B, Fig. 6). Due to the presence of four hydroxyl groups in the compound, the compound is polar and unable to bind at hydrophobic protein surface. Again, 3a is sufficiently hydrophobic because it contains only one OH group and hydrophobic *tert*-butyl group. For this reason, the molecule has low solubility in the buffer medium.

In the presence of insulin, having few hydrophobic pocket on the protein surface, become a host for both ANS and 3a. Due to lower solubility and higher binding ability of 3a with respect to the ANS, the molecule will move from polar aqueous medium to hydrophobic protein sites which will replace ANS from their binding site on insulin. It is evident from the decrease of ANS intensity. However, for the presence of four hydroxyl group in 3b, it is sufficiently hydrophilic and has lesser tendency to replace ANS from their binding sites. Therefore, 3b have different binding site than 3a which is polar in nature. The slight decrease in the ANS fluorescence intensity may be due to the ANS displacement from their binding sites for the conformational change of the protein during 3b binding to the protein. To confirm the results obtained in different studies, the circular dichroism (CD) spectroscopy was employed for monitoring the secondary structural changes.

### Circular dichroism (CD) spectroscopy

Circular dichroism (CD) of a protein gives indications of the secondary and tertiary structural change of the investigating protein. Insulin is an  $\alpha$ -helix enriched protein which shows peak at 208 nm in far-UV CD spectral regions for its  $\alpha$ -helical



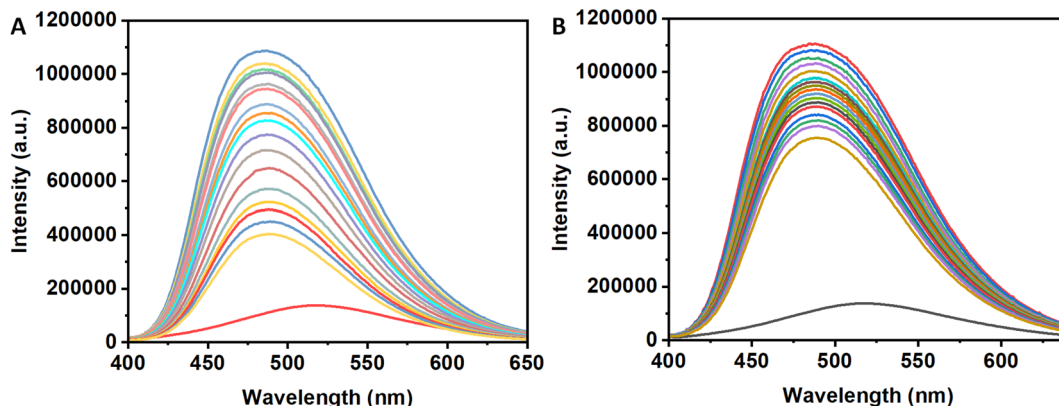


Fig. 6 ANS-fluorescence emission spectra of monomeric insulin incubated separately at 25 °C and at pH 2.0 in the absence and presence of Schiff base **3a** (Panel A) and in the absence and presence of Schiff base **3b** (Panel B). Insulin concentrations throughout all the experiments were kept at 25  $\mu$ M. Results were the average of three different experiments.

structure. If a small molecule such as a Schiff base interacts with the protein and is able to perturb the secondary structure of the insulin, then there will be a change or shift of these peaks. The purified monomeric insulin (6  $\mu$ M) shows peaks at 208 nm and 221 nm which are the characteristic peaks of an alpha helix containing protein like insulin along with the presence of beta sheet structure. For a solution containing insulin and the compound **3a** (1  $\mu$ M), a significant change of far-UV CD spectrum was observed in the above-mentioned peak indicating that the binding of the compound to the protein unable to cause a major change of the secondary structure of the protein (Fig. 7). But addition of higher concentration of **3a** (2 and 6  $\mu$ M) changes the CD spectral pattern of insulin giving higher percent of random structure (Table S1†). Thus the hydrophobic compound **3a** interacts with insulin and perturbs strongly its secondary structure. However, the compound **3b** at

its lower concentration (1 and 2  $\mu$ M) interacts with insulin shows red-shift of these peaks with greater negative ellipticity value compared to monomeric insulin. CD structural analysis shows the formation of slight higher content of  $\beta$ -structure. The difference in MRE value can be related to the structure of the two molecules **3a** and **3b**. At higher concentration of the **3b**, structural transition of insulin was observed. It showed lesser MRE value at 215 nm and increased MRE at 207 nm compared to insulin alone. Thus the hydrophilic compound **3b** has influences in the secondary structure as well as the tertiary structure of the insulin.

Protein function is very much related to the structure of the protein. The results indicate that hydrophobic molecule **3a** has a high potential for the destruction of the secondary structure of insulin in comparison with hydrophilic molecule **3b**. Therefore, the study shows that the stability of insulin is highly dependent on the hydrophilic and hydrophobic environment.

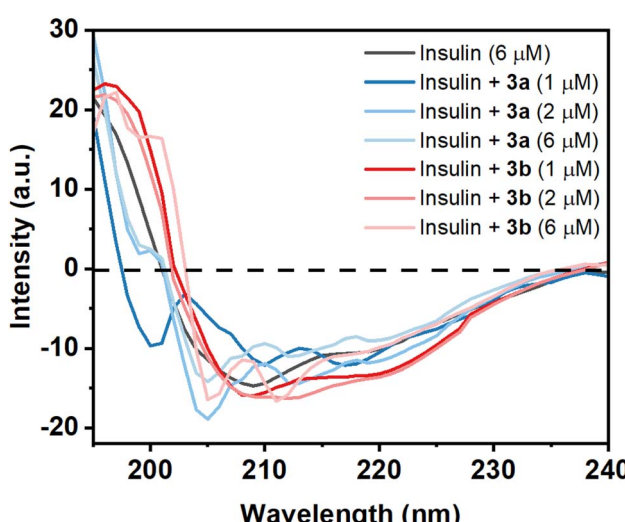


Fig. 7 Far-UV CD spectra (190–250 nm) of monomeric insulin in the absence and presence two small molecules (Schiff bases) **3a** and **3b** at 25 °C and at pH 2.0, showing the secondary structural changes of insulin.

### Theoretical studies

Structural investigation of the Schiff bases will provide significant insight into the nature of the molecule and the contribution of the functional groups to the properties. The molecular electrostatic potential map (MEP) of the energy-minimized structure (using density functional theory (DFT)) of the Schiff bases can provide its electronic distribution around the molecular backbone. Color-coding of the map indicates electron-rich (red), neutral (green), and electron-poor (blue) regions. The **3a** molecule has methoxy and phenolic oxygen and imine nitrogen as polar atoms, whereas **3b** has three additional hydroxyl groups (Fig. 8). All these groups can form an H-bond with protein through either H-bond donation or acceptance depending upon the group. The MEP of both compounds shows a red color on oxygen atoms. It is interesting to notice that the nitrogen atoms are buried in the neutral region. Therefore, imine nitrogen is less capable of H-bond formation.

The polar surface area of **3a** was calculated to be 41.82  $\text{\AA}^2$ , whereas the value was 102.51  $\text{\AA}^2$  for **3b**. Therefore, **3b** has more than double the polar surface area than that of **3a**. For this



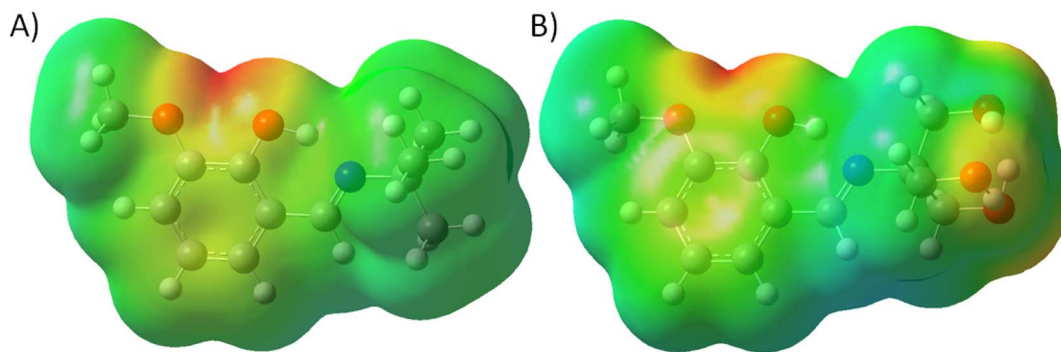


Fig. 8 Molecular electrostatic map of (A) 3a and (B) 3b.

reason, the lipophilicity of **3a** ( $\log P_{o/w} = 2.83$ ) is higher than ( $\log P_{o/w} = 1.73$ ). Again, both the compounds are somewhat water soluble and the  $\log S$  of **3a** and **3b** were calculated to be  $-2.41$  and  $-0.48$ , respectively. For such small molecules, these parameters indicate that they have the potential to form H-bonds with molecules and enough polar.

Molecular docking is one of the most fascinating computational techniques which is used to predict the binding site of a small molecule to a protein, mechanism of protein binding, and weak forces involved in such binding process.<sup>34–36</sup> Here, this

method has been used to predict the binding mode of **3a** and **3b** in the human insulin. The structure of the molecules was energy minimized with the help of density functional theory (DFT). The molecular docking of these compounds to the human insulin showed that the compound **3b** have higher binding affinity with respect to the **3a**. The change of free energy for this binding process is  $-6.83$  and  $-5.74$  kcal mol $^{-1}$  for **3b** and **3a**, respectively. It indicates that the compound **3b** have more binding affinity to the human insulin than **3a** which was also observed experimentally.

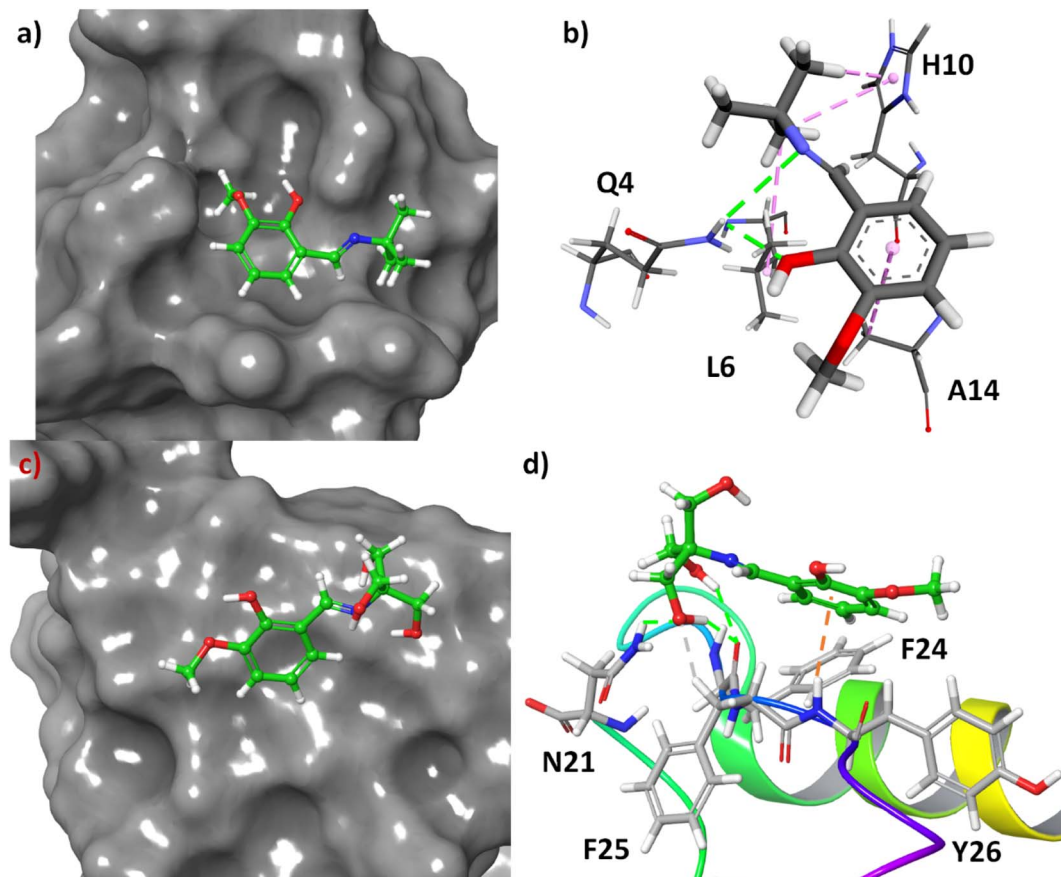


Fig. 9 (a) Docking pose of **3a** in the hydrophobic pocket of the insulin, (b) different non-covalent interactions between **3a** and active site amino acids, (c) docking pose of **3b** on the surface of insulin, (d) different non-covalent interactions in the binding site of the protein with **3b**.



The molecular docking showed that the compound **3a** has been bound at the hydrophobic cavity on the protein surface whereas the **3b** attached at the surface of the protein (Fig. 9, Panel A and Panel B). In the binding process of the **3a**, the amino acid residues Q4, L6, H10, and A14 are involved (Fig. 9C). In the case of **3b**, the binder amino acids are Q21, F24, F25, and Y26 (Fig. 9D). In the binding sites, the N–H of amide group have hydrogen bond with the imine and hydroxyl group of **3a**, imidazole ring of H10 shows C–H···π interactions with *t*-butyl group of **3a**, the methyl group of A14 interact with C–H···π to the benzene ring of **3a**, and L6 interact through hydrophobic interaction with *t*-butyl group of **3a**. However, hydrogen bonding is the main driving forces for the binding of **3b** to the insulin. Amide C=O of F25 involved in hydrogen bonding with two hydroxyl groups at the side-chain of **3b**. Another hydrogen bonding was found to be between amide N–H of N21 and the side-chain OH. The aliphatic C–H of F25 involved in non-conventional H-bonding interactions with the said OH group. Amide N–H of Y26 showed N–H···π interactions with benzene ring of **3b**.

## Experimental

### Materials

Human insulin, marketed by Eli Lilly, India under the trade name 'Huminsulin' was purchased from medicine shop. Few chemicals such as *o*-vanillin, tris(hydroxymethyl)aminomethane, *tert*-butyl amine were procured from Sigma-Aldrich, USA; acetic acid and HCl were purchased from Merck, Germany. Different fluorescent probes, namely 8-anilinonaphthalene-1-sulfonic acid ammonium salts (ANS), thioflavin T (ThT) were purchased from Sigma Chemical (St. Louis, USA). All the other reagents used in our experiments were of analytical grade or of high purity reagent available.

### Preparation and purification of monomeric state of insulin

The hexameric state of insulin marketed as 100 IU mL<sup>-1</sup> equivalent to 2 mg mL<sup>-1</sup> contains the preservative *m*-cresol, tonicity modifier glycerin and pH adjusting substances HCl/NaOH. However, through extensive dialysis with water, these substances were successfully removed. In the next step, 80% acetic acid was added to convert it to a monomer state with a final concentration of 20%. To ensure the formation of amyloid-like fibrils, the solution was filtered through a 0.22 μm (Millipore) filter membrane to remove traces of hexameric molecules. The filtrate was then kept at 37 °C overnight, resulting in a homogeneous solution serving as the monomeric state of insulin (1.5 mg mL<sup>-1</sup>). An optical value of  $\epsilon$  (276 nm) = 10.0 was considered in this process.

### Synthesis of **3a** and **3b**

In a 10 mL round-bottomed flask equipped with a condenser and stirring bar, a mixture of ethanol (3 mL), *ortho*-vanillin (1.0 mmol), amine (1.2 mmol) and one drop of acetic acid was prepared. Upon addition of the components, the reaction mixture turned yellow in color. The mixture was then refluxed

for three hours with stirring and subsequently allowed to cool to room temperature. To the cooled mixture, 10 mL of water was added and the resulting mixture was extracted with CH<sub>2</sub>Cl<sub>2</sub> (3 × 5 mL). The combined organic layer was dried over anhydrous Na<sub>2</sub>SO<sub>4</sub> and evaporated in vacuum. Finally, the compounds obtained were purified by either crystallization or column chromatography, followed by crystallization. The <sup>1</sup>H and <sup>13</sup>C NMR of the products (observed in DMSO-d<sub>6</sub>) can be found in ESI File (Fig S5–S8).†

### UV-visible spectroscopy

We utilized a JASCO Spectrophotometer model no. V700 (Serial No. B184461798) at room temperature (25 °C) to measure precisely the absorbance and determined the binding affinity and binding constants. UV titrations were conducted by gradually increasing the concentrations of insulin (1–20 μM) for **3a** and (1–20 μM) for **3b** in a 1 cm quartz cuvette that contained a constant concentration of **3a** and **3b** (20 μM) in Milli-Q water. The spectra were recorded between 200–600 nm. To check the stability of the compounds, they were subject to under investigation through UV-vis spectroscopy in water at 20 μM separately with respect to time.

### Intrinsic fluorescence study of insulin in presence of Schiff base compounds

The study conducted fluorescence quenching experiments using HORIBA (Model: FLUOROMAX-4C, serial no. 1734D-4018-FM) at room temperature after exciting the solutions at 276 nm and following the emission in the wavelength range 290–400 nm and keeping the excitation and emission slits at 5 nm. The concentration of insulin was kept constant at 25 μM while **3a** and **3b** were added successively from 2 to 24 μM and 2 to 24 μM, respectively. The excitation wavelength for **3a** and **3b** derivative was 335 nm and 325 nm, respectively, and emission was recorded between 350–550 nm. To understand the spectroscopic behaviour of both the compounds, concentration dependent fluorescence spectroscopy was recorded in water at the said excitation wavelength.

### ANS assay for monitoring the hydrophobicity changes

The hydrophobicity of protein molecules was determined by employing a fluorescent probe that binds to the hydrophobic pockets on the protein 1-anilinonaphthalene-8-sulfonate (ANS) is a well-known polarity sensitive probe that shows specific binding with the hydrophobic pockets. A stock solution of ANS was prepared and mixed to 2 mL monomeric insulin samples to determine hydrophobicity. The final ANS concentration in each sample aliquot was kept constant at 30 μM. The protein samples were then treated with **3a** and **3b** chemicals at doses ranging from 2 to 60 μM and 2 to 60 μM, respectively. Shimadzu Spectrofluorometer (Shimadzu 5301 PC) was used to record the emission spectra from 390 to 600 nm after excitation at 350 nm. The length of the path was 1 cm. Both the excitation and emission slits were set at 5 nm.



## Circular dichroism (CD) spectroscopy

We recorded far-UV CD spectra of insulin in the presence of the Schiff bases **3a** and **3b** using a Jasco spectropolarimeter (Model: J-815). The measurements were done in a nitrogen atmosphere, with a quartz cell of path length 0.2 cm in the far-UV region (200–260 nm). We maintained a constant concentration of insulin at 6  $\mu$ M, while the concentrations of **3a** and **3b** derivatives were varied (1–6  $\mu$ M). We collected data for each nm from 260 to 200 nm at a scan speed of 50 nm per minute. The sample temperature was kept at 25 °C using a Neslab RTE-111 circulating water bath connected to water-jacketed quartz cuvettes. To calculate the secondary structures of insulin, we utilized CDNN 2.1 software attached with the instrument.

## Molecular docking

The RCSB Protein Data Bank website (PDB ID: 3I40) provided us with the crystal structure of human insulin. We thoroughly analyzed this biopolymer's structure and prepared it for a docking experiment. Our team optimized the structures of **3a** and **3b** using the Density Functional Theory (DFT) B3LYP/6-31G level of theory to minimized energy. For MEP, a same functional and basis sets have been utilized. These optimized structures were then used for docking with insulin protein to identify the most probable site and mode of binding using the grid-based docking program Auto Dock 4.2. To ensure accuracy, we removed the ligand present in the protein and water molecules from the protein and assigned Atom Kollman charges after adding polar hydrogen for the protein. We utilized the default parameters of Auto Dock and the generic algorithm to conduct this calculation. The visualization effects were expertly prepared using Discovery Studio 4.1 Client. We are confident in the accuracy and validity of our findings. The polar surface area, lipophilicity, and water solubility was predicted using SwissADMET.<sup>37</sup>

## Conclusions

In conclusion, the effects of hydrophilic and hydrophobic molecules on the insulin binding process have been investigated through a multi-spectroscopic approach. We have synthesized two Schiff base molecules with hydrophilic and hydrophobic side chains. The findings of our investigation show that glucose (hydrophilic) binding protein insulin has also a sufficient affinity to bind with the hydrophobic molecules. The binding constant of hydrophobic and hydrophilic molecules was found to be  $4.99 \times 10^4 \text{ M}^{-1}$  and  $6.64 \times 10^4 \text{ M}^{-1}$ , respectively, at 283 K. The binding of hydrophobic molecules at the hydrophobic pocket of insulin perturbs greatly the secondary structure of the monomeric insulin whereas the hydrophilic molecule causes small alterations in the secondary structural contents on binding with insulin. Thus, stability of insulin is diminished in the presence of hydrophobic molecules.

## Conflicts of interest

The authors declare no competing financial interest.

## Acknowledgements

Financial support of Indian Council of Medical Research (ICMR), Govt. of India, is greatly acknowledged. Shahnaz Begum is the recipient of ICMR-SRF fellowship. Financial support of University Grants Commission UGC-CAS-II and DST-PURSE-II (Govt. of India) Program of Department of Chemistry, Jadavpur University, Kolkata are also acknowledged. Dr Mohd Afzal extends his appreciation to Researchers Supporting Project Number (RSPD2023R979), King Saud University, Riyadh, Saudi Arabia, for financial assistance.

## References

- 1 S. C. Bagley and R. B. Altman, *Protein Sci.*, 2008, **4**, 622–635.
- 2 V. H. Nguyen and B.-J. Lee, *Int. J. Nanomed.*, 2017, **12**, 3137–3151.
- 3 R. Sinha and S. K. Khare, *Front. Microbiol.*, 2014, **5**, 165.
- 4 H.-X. Zhou and X. Pang, *Chem. Rev.*, 2018, **118**, 1691–1741.
- 5 L. Mabonga and A. P. Kappo, *Biophys. Rev.*, 2019, **11**, 559–581.
- 6 D. K. Ghosh and A. Ranjan, *Protein Sci.*, 2020, **29**, 1559–1568.
- 7 L. M. Stevers, E. Sijbesma, M. Botta, C. MacKintosh, T. Obsil, I. Landrieu, Y. Cau, A. J. Wilson, A. Karawajczyk, J. Eickhoff, J. Davis, M. Hann, G. O'Mahony, R. G. Doveston, L. Brunsved and C. Ottmann, *J. Med. Chem.*, 2018, **61**, 3755–3778.
- 8 V. Corradi, B. I. Sejdiu, H. Mesa-Galloso, H. Abdizadeh, S. Y. Noskov, S. J. Marrink and D. P. Tieleman, *Chem. Rev.*, 2019, **119**, 5775–5848.
- 9 E. Hallacli, C. Kayatekin, S. Nazeen, X. H. Wang, Z. Sheinkopf, S. Sathyakumar, S. Sarkar, X. Jiang, X. Dong, R. Di Maio, W. Wang, M. T. Keeney, D. Felsky, J. Sandoe, A. Vahdatshoar, N. D. Udeshi, D. R. Mani, S. A. Carr, S. Lindquist, P. L. De Jager, D. P. Bartel, C. L. Myers, J. T. Greenamyre, M. B. Feany, S. R. Sunyaev, C. Y. Chung and V. Khurana, *Cell*, 2022, **185**, 2035–2056.
- 10 G. Wilcox, *Clin. Biochem. Rev.*, 2005, **26**, 19–39.
- 11 M. S. Rahman, K. S. Hossain, S. Das, S. Kundu, E. O. Adegoke, M. A. Rahman, M. A. Hannan, M. J. Uddin and M.-G. Pang, *Int. J. Mol. Sci.*, 2021, **22**, 6403.
- 12 B. M. Y. Cheung and C. Li, *Curr. Atheroscler. Rep.*, 2012, **14**, 160–166.
- 13 W. Fan, *Cardiovasc. Endocrinol.*, 2017, **6**, 8–16.
- 14 R. Chen, B. Ovbiagele and W. Feng, *Am. J. Med. Sci.*, 2016, **351**, 380–386.
- 15 E. Giovannucci, D. M. Harlan, M. C. Archer, R. M. Bergenstal, S. M. Gapstur, L. A. Habel, M. Pollak, J. G. Regensteiner and D. Yee, *Diabetes Care*, 2010, **33**, 1674–1685.
- 16 I. Martín-Timón, *World J. Diabetes*, 2014, **5**, 444.
- 17 T. N. Vinther, M. Norrman, U. Ribel, K. Huus, M. Schlein, D. B. Steensgaard, T. Å. Pedersen, I. Pettersson, S. Ludvigsen, T. Kjeldsen, K. J. Jensen and F. Hubálek, *Protein Sci.*, 2013, **22**, 296–305.
- 18 N. Nagel, M. A. Graewert, M. Gao, W. Heyse, C. M. Jeffries, D. Svergun and H. Berchtold, *Biophys. Chem.*, 2019, **253**, 106226.



19 C. L. Maikawa, A. A. A. Smith, L. Zou, C. M. Meis, J. L. Mann, M. J. Webber and E. A. Appel, *Adv. Ther.*, 2020, **3**, 1900094.

20 A. D. G. Lawson, M. MacCoss and J. P. Heer, *J. Med. Chem.*, 2018, **61**, 4283–4289.

21 R. R. Thangudu, S. H. Bryant, A. R. Panchenko and T. Madej, *J. Mol. Biol.*, 2012, **415**, 443–453.

22 S. Chaturvedi, P. P. Hazari, A. Kaul, Anju and A. K. Mishra, *ACS Omega*, 2020, **5**, 26297–26306.

23 S. Zhong, J.-H. Jeong, Z. Chen, Z. Chen and J.-L. Luo, *Transl. Oncol.*, 2020, **13**, 57–69.

24 H. Schiff, *Ann. Chem. Pharm.*, 1864, **131**, 118–119.

25 M. G. Humphrey, T. Schwich, P. J. West, M. P. Cifuentes and M. Samoc, in *Comprehensive Inorganic Chemistry II*, Elsevier, 2013, pp. 781–835.

26 C. J. Burns, M. P. Neu, H. Boukhalfa, K. E. Gutowski, N. J. Bridges and R. D. Rogers, in *Comprehensive Coordination Chemistry II*, Elsevier, 2003, pp. 189–345.

27 W. Wang, R. Narain and H. Zeng, in *Polymer Science and Nanotechnology*, Elsevier, 2020, pp. 203–244.

28 Y. Dong and W. Wang, in *Wound Healing Biomaterials*, Elsevier, 2016, pp. 289–307.

29 H. Liu, S. Ding, Q. Lu, Y. Jian, G. Wei and Z. Yuan, *ACS Omega*, 2022, **7**, 7585–7594.

30 P. Patel, K. Parmar and M. Das, *Int. J. Biol. Macromol.*, 2018, **108**, 225–239.

31 P. Alam, A. Z. Beg, M. K. Siddiqi, S. K. Chaturvedi, R. K. Rajpoot, M. R. Ajmal, M. Zaman, A. S. Abdelhameed and R. H. Khan, *Arch. Biochem. Biophys.*, 2017, **621**, 54–62.

32 A. Das, Y. M. Gangarde, V. Tomar, O. Shinde, T. Upadhyay, S. Alam, S. Ghosh, V. Chaudhary and I. Saraogi, *Mol. Pharm.*, 2020, **17**, 1827–1834.

33 S. Das and D. Bhattacharyya, *J. Cell. Biochem.*, 2017, **118**, 4881–4896.

34 N. Sepay, P. C. Saha, Z. Shahzadi, A. Chakraborty and U. C. Halder, *Phys. Chem. Chem. Phys.*, 2021, **23**, 7261–7270.

35 N. Sepay, N. Sepay, A. Al Hoque, R. Mondal, U. C. Halder and M. Muddassir, *Struct. Chem.*, 2020, **31**, 1831–1840.

36 N. Sepay, S. Chakrabarti, M. Afzal, A. Alarifi and D. Mal, *RSC Adv.*, 2022, **12**, 24178–24186.

37 A. Daina, O. Michielin and V. Zoete, *Sci. Rep.*, 2017, **7**, 42717.

